SolarPACES 2024, 30th International Conference on Concentrating Solar Power, Thermal, and Chemical Energy Systems

Thermal Energy Storage Materials, Media, and Systems

https://doi.org/10.52825/solarpaces.v3i.2297

Published: 19 Nov. 2025

Numerical Simulation to Investigate Thermal Stratification in an Energy Storage System Under No-Flow Condition

Kapil Kumar[1,*], Shireesh B. Kedare[1], and Manaswita Bose[1]

[1]Department of Energy Science and Engineering, Indian Institute of Technology Bombay, Mumbai (India)

*Correspondence: Kapil Kumar, 214170004@iitb.ac.in

Abstract. Thermal energy storage (TES) systems enhance the reliability of intermittent energy sources. The present work examines the thermal stratification in a thermocline storage system during charging and discharging with no fluid flows. With this goal, numerical simulations are performed on a storage tank consisting of a constant temperature heat source and sink. Molten nitrate salts mixture (60 % $NaNO_3$+ 40 % KNO_3) is used as storage material as it is thermally stable at higher temperatures (up to 565 °C). The thermocline behaviour of the numerical model is assessed during charging and discharging using constant temperature heating and cooling sources. In the present study, molten salts' lower and upper-temperature limits are 300 °C and 500 °C, respectively. The qualitative behaviour of thermocline formation and propagation during charging and discharging is analysed by temperature contours and axial temperature profiles. Quantitatively, the thermocline behaviour is analysed by two non-dimensional parameters: Stratification number (Str) and Mix number (MIX). It is observed that with a constant temperature heat source and sink, the tank remains stratified throughout the charging and discharging. The charging and discharging rates have been determined, and the results will be helpful in designing a lab-scale thermocline demonstration setup and further study.

Keywords: Thermal Energy Storage (TES), No-Flow Thermocline Storage System, Stratification Number (Str), Mix Number (MIX), Charging and Discharging Processes.

1. Introduction

Thermal energy storage (TES) has vast applications in process heating and electricity generation in concentrated solar power (CSP) plants [1]. It consists of suitable storage materials for storing surplus or waste heat for further utilization. From the CSP plants' perspective, two well-known thermal energy storage technologies are two-tank and single-tank thermocline storage [2]. Two-tank storage is a mature technology, while single-tank thermocline storage is a state-of-the-art and cost-effective alternative to two-tank storage [3], [4]. In the thermocline storage system, hot and cold fluids remain in the same tank, separated under the buoyancy force, a phenomenon called thermal stratification. Single-tank thermocline storage is categorized as single-media thermocline and dual-media thermocline. It is reported that the single-media thermocline performs better than the dual-media thermocline [5]. Gajbhiye et al. found that the thermocline thickness for a single-media thermocline system with a porous distributor is 40 % less than that of a dual-media thermocline [6].

Numerous other studies have assessed the single media thermocline performance during charging and discharging [7-10]. To demonstrate the high-temperature lab-scale thermocline system behaviour with freezing storage materials (like molten salt), it is recommended to use a no-flow type thermocline system as the continuous heat supply required in a flow-type system. With that objective, the numerical study on a lab-scale computational model is performed with constant temperature heating and cooling sources while the molten salt remains in no-flow conditions. In the study, the authors depict the thermocline formation and propagation with molten salt storage for charging and discharging. It is qualitatively shown by temperature contours and cross-sectional averaged temperature profiles, and quantified by Stratification and Mix numbers. The heating and cooling rates concerning the constant temperature heat source and heat sink are also determined during charging and discharging. The present study is performed primarily to assess the thermocline behaviour of a high-temperature molten salt thermocline system during charging and discharging. Moreover, the study is applicable to storing excess electrical energy into thermal energy for process heating applications and to avail the Time-of-Day tariff for the peak hour's industrial process heat requirements.

2. Methodology: Numerical model, grid, and time-step independence test

The 2D axis-symmetric computational geometry of a thermocline tank is shown in Figure 1a. The constant temperature heat source and heat sink are located near the top and bottom, respectively, with the dimensions provided in Table 1. Further, the grid and time-step independence tests are performed to ensure the grid and time-step independent solutions. The test results are plotted in Figures 1b and 1c; based on the tests, mesh size 3 and a time step of 2 seconds are selected. A mixture of molten nitrate salts (60 % $NaNO_3$+ 40 % KNO_3) is chosen as a thermal energy storage material suitable for high-temperature applications. Temperature-dependent properties of the molten nitrate salt are provided in Table 2 [11]. The temperature limit considered is 300 °C to 500 °C. The simulation software employed is COMSOL Multiphysics version 5.5 to solve the mass conservation, momentum conservation, and energy transport equations for instantaneous temperature profiles. The mass and momentum conservation and energy transport equations are expressed as Equations 1 – 3 [12]. For the charging process, the whole tank is initially kept at a lower limit temperature T_c = 300 °C, and the heat source is kept at an upper limit temperature T_h = 500 °C. For discharging, the tank is initially kept at T_h = 500 °C and the heat sink at T_c = 300 °C.

The temperature contours depict the thermocline formation and propagation at different time steps during charging and discharging. The same can also be observed by the leftward and rightward movement of temperature profiles on temperature versus height plots for the charging and discharging process. The dimensionless parameters Str and MIX are plotted with time for the quantitative measure of the degree of thermal stratification. The stratification number (Str) is the ratio of the mean temperature gradient to the maximum temperature gradient. The expression for Str is provided as Equation 4 [13]. Str's zero and unit values represent a thermocline tank's thoroughly mixed and stratified state. Another parameter to quantify the thermal stratification is the Mix number (MIX), which is defined as the ratio of energy moments difference for a stratified and real tank and that for a stratified and mixed tank. The expression for MIX can be provided as Equation 5 [14]. The energy moments are expressed as Equation 6. All the results are discussed in the subsequent section.

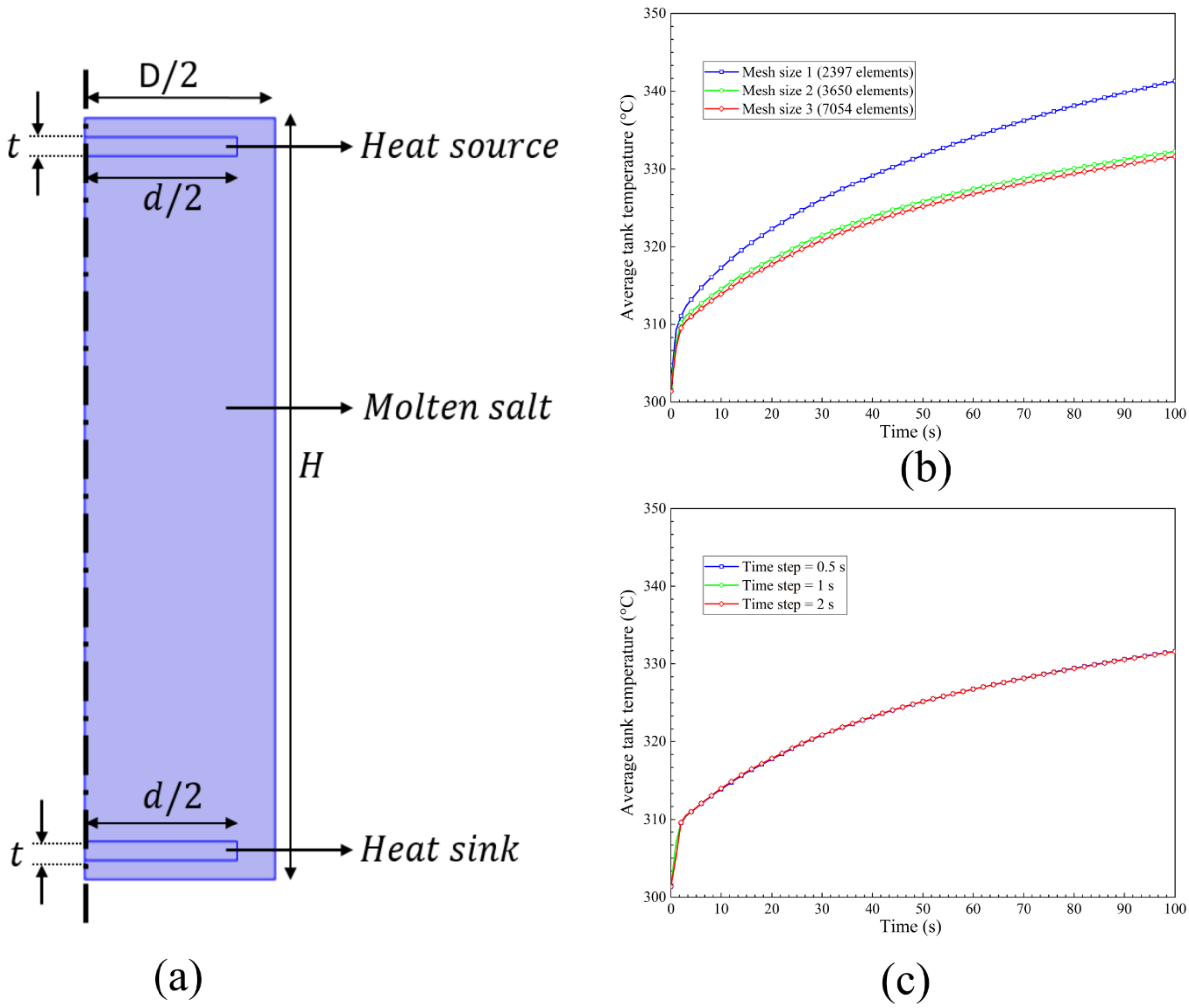

Figure 1. *(a) 2D axis-symmetric computational model, (b) Grid independence test plot, (c) Time-step independence test plot.*

Table 1*. Computational model dimensions.*

Dimension	Value
Tank height (H)	200 mm
Tank diameter (D)	100 mm
Heat source and sink diameter (d)	80 mm
Heat source and sink height (t)	5 mm

Table 2*. Thermophysical properties of molten salt [11].*

Thermophysical property	Expression
Density	$\rho = 2090 - 0.636\,T$
Specific heat	$C_p = 1443 - 0.172\,T$
Thermal conductivity	$k = 0.443 + 1.9 * 10^{-4}\,T$
Dynamic viscosity	$\mu = (22.714 - 0.12\,T + 2.281 * 10^{-4}\,T^2 - 1.474 * 10^{-7}\,T^3) * 10^{-3}$

$$\frac{\partial \rho}{\partial t} + \nabla \cdot (\rho\,\vec{v}) = 0 \tag{1}$$

$$\frac{\partial(\rho\vec{v})}{\partial t} + (\nabla \cdot \rho\,\vec{v}\,\vec{v}) = -\nabla p + \rho\,\vec{g} + \nabla \cdot \mu(\nabla\,\vec{v} + \nabla\,\vec{v}^T) \tag{2}$$

$$\frac{\partial(\rho\, C_p\, T)}{\partial t} + \nabla \cdot \left(\rho\, C_p\, \vec{v}\;\, T\right) = \nabla \cdot (\mathrm{k}\, \nabla\, T) \tag{3}$$

$$Str = \frac{T_{top} - T_{bottom}}{T_h - T_c} \tag{4}$$

$$MIX = \frac{E_{str} - E_{real}}{E_{str} - E_{mix}} \tag{5}$$

$$E = \sum_{i=1}^{n} e_i\, z_i \tag{6}$$

Where $\vec{v}$, T, p, g, ρ, µ, C_p, and k are the velocity vector (m s^{-1}), temperature (°C), pressure (Pa), acceleration due to gravity (m s^{-2}), density (kg m^{-3}), dynamic viscosity (kg m^{-1} s^{-1}), specific heat (J kg^{-1} K^{-1}), and thermal conductivity (W m^{-1} K^{-1}) respectively. T_{top} and T_{bottom} are the thermocline tank's top and bottom layer temperatures. E_{str}, E_{real}, and E_{mix} are the energy moments for a stratified, real, and mixed thermocline tank. Subscript *i* represents the i^{th} layer from the tank bottom, while dividing it into *n* layers, e_i represents the heat content, and z_i represents the height of the i^{th} layer from the bottom.

3. Results and discussion

Temperature contours for the charging and discharging processes are depicted in Figures 2a and 2b, respectively. Figure 2a shows that as the heater starts supplying heat at a constant temperature, the hot molten salt remains in the top portion of the tank under buoyancy forces. As the charging time progresses, more and more salt gets heated, and the transition zone between hot and cold salt starts moving downward, as shown in Figure 2a. The transition zone moves upward during discharging, as demonstrated in Figure 2b. The cross-sectional averaged temperature profiles for the charging and discharging process are provided in Figures 3a and 3b, respectively. The temperature profile in the transition zone is observed to be near sigmoidal, moving leftwards and rightwards as the charging and discharging time progresses.

Figures 4a and 4b depict the variation of the Stratification number with time for charging and discharging processes. At the start of charging, the tank is at the lower temperature limit T_c, corresponding to its mixed state with zero Str value. As the charging time passes, the Str value increases and achieves a plateau near unity. This tells that the tank remains stratified during the entire charging process, and at the end of charging, the Str value declines to zero as it achieves a mixed state at the upper-temperature limit T_h. The Str plot for the discharging process (Figure 4b) also shows that the Str value is zero at the start of discharging. It increases and achieves a near unity value to confirm that the tank remains stratified during discharging. The Mix number plots for charging and discharging processes are shown in Figures 5a and 5b. This gives a more detailed measurement of the degree of stratification inside the thermocline tank. The MIX plots for the charging and discharging processes corroborate with the Str plots and show that the tank remains stratified during the entire charging and discharging process. With time, the MIX value increases as the thermal diffusion increases. The variation of heating and cooling rates during the charging and discharging process with time is shown in Figures 6a and 6b. The plots depict that the charging rate is initially higher due to more significant temperature gradients, and later, it declines. It is observed that for the said tank geometry (0.22 kWh capacity), the maximum heating rate and cooling rate are 1.06 kW and 1.13 kW, respectively.

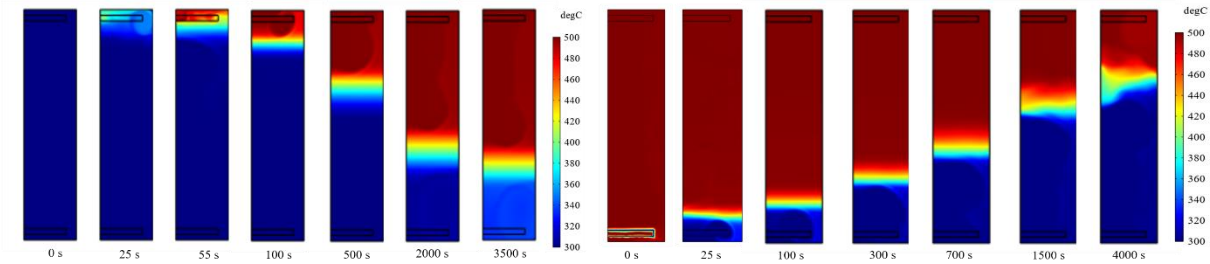

(a) (b)

Figure 2. *(a) Temperature contours during the charging process, (b) Temperature contours during the discharging process.*

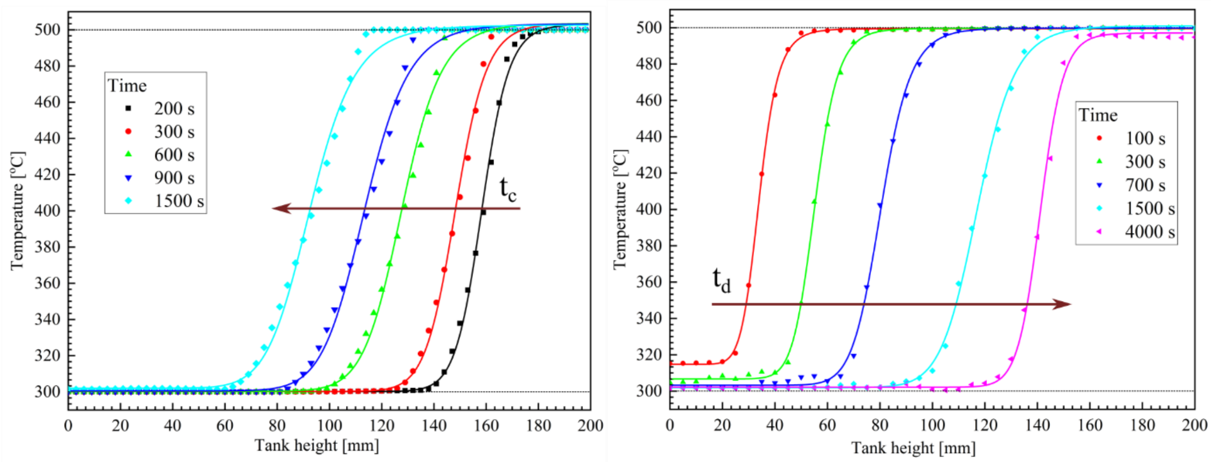

(a) (b)

Figure 3. *(a) Temperature profiles during charging process, (b) Temperature profiles during discharging process.*

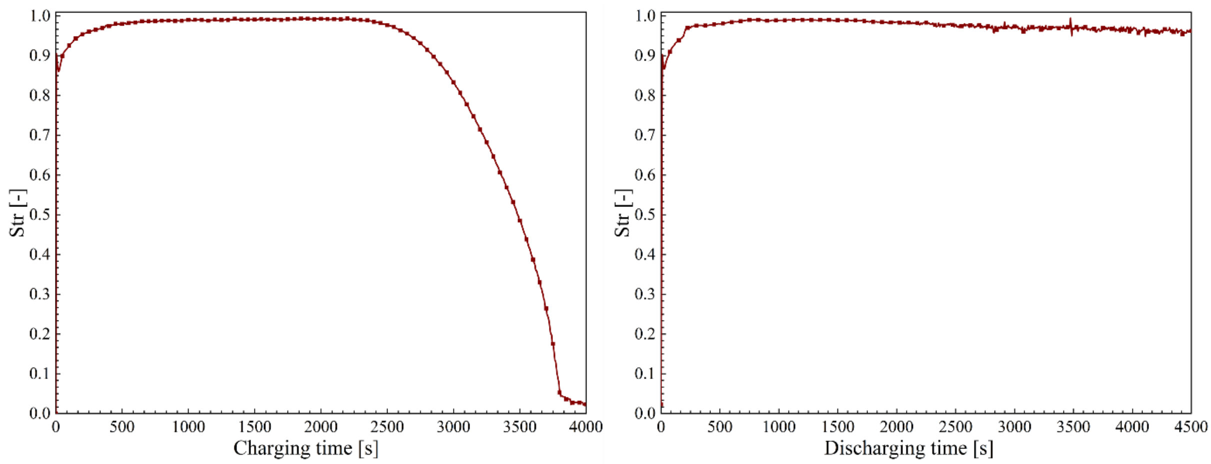

(a) (b)

Figure 4*. (a) Variation of Stratification number with charging time, (b) Variation of Stratification number with discharging time.*

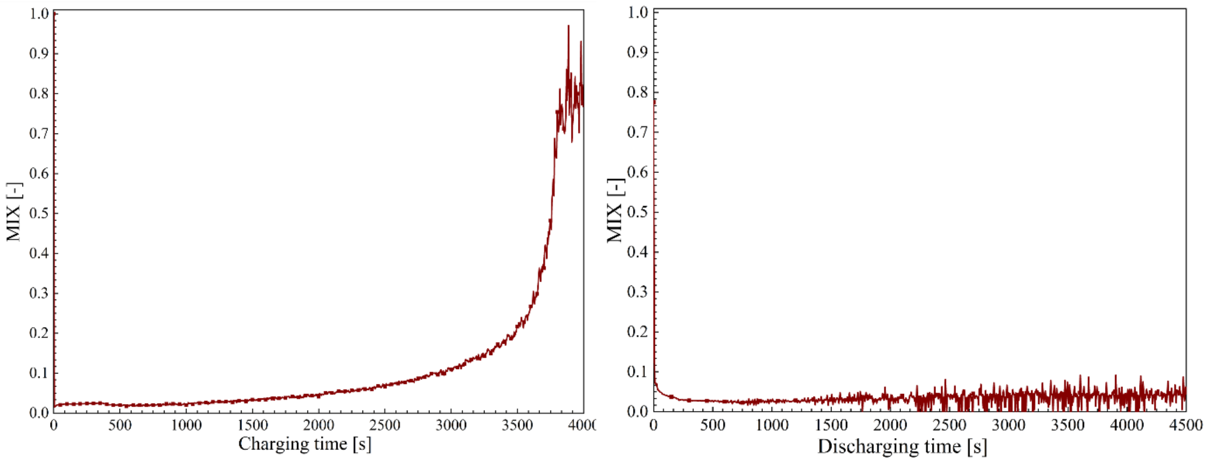

(a) (b)

Figure 5. *(a) Variation of Mix number with charging time, (b) Variation of Mix number with discharging time.*

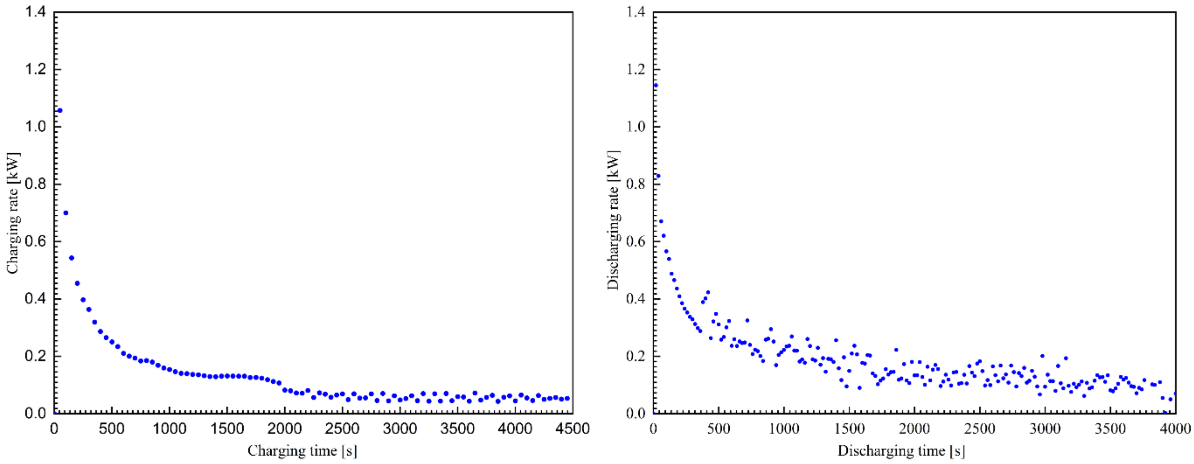

(a) (b)

Figure 6. *(a) Variation of charging rate with time, (b) Variation of discharging rate with time.*

4. Conclusions

In the present study, the charging and discharging behaviour of a thermocline storage tank with a constant temperature heat source and sink is simulated. The temperature contours, axial temperature profile, Str, and Mix are used to assess the thermocline behaviour, and the heating and cooling rates are also determined. The temperature profiles for both processes are sigmoidal and similar to the standard thermocline storage systems, so the flow-type thermocline can be mimicked. The Stratification and mix number plots depict that the tank remains stratified for charging and discharging under the action of dominant buoyancy forces. Also, the tank remains stratified in idle conditions for prolonged periods. The maximum charging and discharging rates for the storage tank with said geometry (0.22 kWh capacity) are 1.06 kW and 1.13 kW, respectively.

The findings from the study can be used to design the lab-scale molten-salt thermocline demonstration setup for a variable charging-discharging and losses study. Other applications of the present study are storing excess electrical energy as thermal energy for process heating applications. Also, to avail the Solar Time-of-Day tariff for the peak hours' industrial process heat requirements.

Data availability statement

Data sharing is not applicable.

Author contributions

Kapil Kumar: Conceptualization, Methodology, Software, Data curation, Investigation, Visualization, Writing-original draft.

Shireesh B Kedare: Resources, Conceptualization, Methodology, Visualization, Supervision, Writing-review and editing.

Manaswita Bose: Resources, Conceptualization, Methodology, Visualization, Supervision, Writing-review and editing.

Competing interests

The authors declare that they have no competing interests.

Acknowledgement

The authors are thankful to the Indian Institute of Technology Bombay for providing the licensed version of COMSOL Multiphysics version 5.5, MATLAB, and Grammarly to enhance the clarity of writing. Also, I am grateful to the Prime Minister Research Fellowship (PMRF) committee for awarding the fellowship and contingency for necessary resources.

References

[1] A. Palacios, C. Barreneche, M. Navarro, and Y. Ding, “Thermal energy storage technologies for concentrated solar power–a review from a materials perspective,” Renewable Energy, vol. 156, pp. 1244–1265, 2020. DOI: https://doi.org/10.1016/j.renene.2019.10.127.

[2] R. Bay´on and E. Rojas, “Simulation of thermocline storage for solar thermal power plants: From dimensionless results to prototypes and real-size tanks,” International Journal of Heat and Mass Transfer, vol. 60, pp. 713–721, 2013. DOI: https://doi.org/10.1016/j.ijheatmasstransfer.2013.01.047.

[3] J.E.Pacheco, S.K.Showalter, and W. J. Kolb, “Development of a molten-salt thermocline thermal storage system for parabolic trough plants,” J. Sol. Energy Eng., vol. 124, no. 2, pp. 153–159, 2002. DOI: https://doi.org/10.1115/1.1464123.

[4] K. Kumar, V. Joshi, S. B. Kedare, and M. Bose, “Performance assessment of a porous flow distributor in arresting the effect of temperature fluctuation in a thermocline system,” Thermal Science and Engineering Progress, vol. 55, p. 102942, 2024. DOI: https://doi.org/10.1016/j.tsep.2024.102942.

[5] C. Mira-Hern´andez, S. Flueckiger, and S. Garimella, “Numerical simulation of single- and dual-media thermocline tanks for energy storage in concentrating solar power plants,” Energy Procedia, vol. 49, pp. 916–926, 2014. DOI: https://doi.org/10.1016/j.egypro.2014.03.099.

[6] P. Gajbhiye, N. Salunkhe, S. Kedare, and M. Bose, “Experimental investigation of single media thermocline storage with eccentrically mounted vertical porous flow distributor,” Solar Energy, vol. 162, pp. 28–35, 2018. DOI: https://doi.org/10.1016/j.solener.2017.12.062.

[7] W. Shaikh, A. Wadegaonkar, S. Kedare, and M. Bose, "Numerical simulation of single media thermocline based storage system," Solar Energy, vol. 174, pp. 207–217, 2018. DOI: https://doi.org/10.1016/j.solener.2018.08.084.

[8] P. Gajbhiye, S. Kedare, and M. Bose, "Experimental analysis of parameters influencing thermal stratification in single media single tank storage system with flow distributor," Thermal Science and Engineering Progress, vol. 30, p. 101243, 2022. DOI: https://doi.org/10.1016/j.tsep.2022.101243.

[9] V. Joshi, C. Wasnik, A. Wadegaonkar, S. B. Kedare, and M. Bose, "Influence of porosity and permeability of flow distributor on thermal stratification in single media storage tank," Journal of Energy Storage, vol. 44, p. 103241, 2021. DOI: https://doi.org/10.1016/j.est.2021.103241.

[10] K. Kumar and S. Singh, "Investigating thermal stratification in a vertical hot water storage tank under multiple transient operations," Energy Reports, vol. 7, pp. 7186–7199, 2021. DOI: https://doi.org/10.1016/j.egyr.2021.10.088.

[11] C.Xu, Z. Wang, Y. He, X. Li, and F. Bai, "Sensitivity analysis of the numerical study on the thermal performance of a packed-bed molten salt thermocline thermal storage system," Applied Energy, vol. 92, pp. 65–75, 2012. DOI: https://doi.org/10.1016/j.apenergy.2011.11.002.

[12] "Comsol 2019. multiphysics reference guide for comsol 5.5." (2019), [Online]. Available: https://doc.comsol.com/5.5/doc/com.comsol.help.comsol/COMSOL_ReferenceManual.pdf (visited on 08/15/2024).

[13] J. Fernandez-Seara, F. J. Uhı, J. Sieres, et al., "Experimental analysis of a domestic electric hot water storage tank. part ii: Dynamic mode of operation," Applied thermal engineering, vol. 27, no. 1, pp. 137–144, 2007. DOI: https://doi.org/10.1016/j.applthermaleng.2006.05.004.

[14] J. H. Davidson, D. Adams, and J. Miller, "A coefficient to characterize mixing in solar water storage tanks," 1994. DOI: https://doi.org/10.1115/1.2930504.